

Fermi Energy Level Tuning for High Performance Dye Sensitized Solar Cell Using sp^2 Selective Nitrogen-Doped Carbon Nanotube Channels

Ga In Lee,^a Narayan Chandra Deb Nath,^b Subrata Sarker,^b Weon Ho Shin,^a A. J. Saleh Ahammad,^b Jeung Ku Kang,^{*a} and Jae-Joon Lee,^{*b}

⁵ Received (in XXX, XXX) Xth XXXXXXXXXX 20XX, Accepted Xth XXXXXXXXXX 20XX

DOI: 10.1039/b000000x

Supplementary Information

10

Table S1. Open circuit voltages (V_{oc}), short circuit current densities (J_{sc}) on **SI**, **SII**, and **SIII** arrangements. Concentrations of pristine-CNTs were 0.9, 0.2, 0.025, and 0.01 % (w/w) with respect to TiO₂. For **SII**, nanotubes were electrodeposited by applying 25 V for 10 min.

Content of CNTs (% w/w)	Electrode	V_{oc} (V)	J_{sc} (mA/cm ²)	FF (%)	η (%)
0	Reference	0.75	1.05	70.1	0.55
0.01	SI	0.73	1.08	69.5	0.548
	SIII	0.75	1.05	67.1	0.530
0.025	SI	0.72	1.25	68.9	0.620
	SIII	0.75	1.22	68.5	0.624
0.2	SI	0.69	0.95	70.0	0.458
	SIII	0.70	1.03	69.7	0.504
0.9	SI	0.66	0.87	66.6	0.384
	SIII	0.67	1.00	71.7	0.482
Pure CNTs by electrodeposition	SII	0.70	1.23	56.7	0.484

20

Table S2 Open circuit voltages (V_{oc}), short circuit current densities (J_{sc}) on **SI**, **SII**, and **SIII** arrangements. Concentrations of N(sp^2)-CNTs were 0.9, 0.2, 0.025, and 0.01 % (w/w) with respect to TiO_2 . For **SII**, nanotubes were electrodeposited by applying 25 V for 10 min.

Contents of N(sp^2)-CNTs (% w/w)	Electrode	V_{oc} (V)	J_{sc} (mA/cm ²)	FF (%)	η (%)
0	Reference	0.75	1.05	70.1	0.55
0.01	SI	0.75	1.05	70.5	0.56
	SIII	0.76	1.06	68.2	0.55
0.025	SI	0.75	1.28	68.5	0.66
	SIII	0.75	1.26	70.5	0.67
0.2	SI	0.74	0.96	67.7	0.48
	SIII	0.75	1.03	69.9	0.54
0.9	SI	0.74	0.89	67.2	0.44
	SIII	0.74	1.02	71.6	0.53
N(sp^2)-CNTs by electrodeposition	SII	0.74	1.15	66.0	0.56

5

10

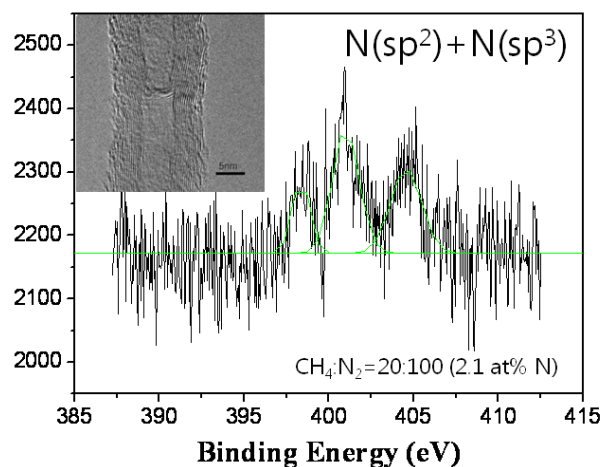
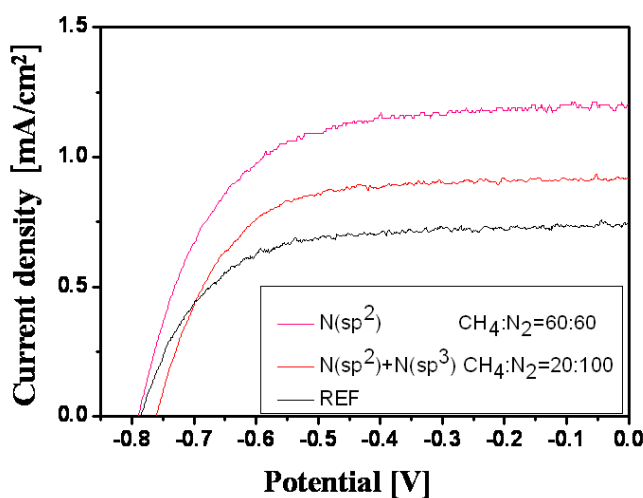
15

20

25

30

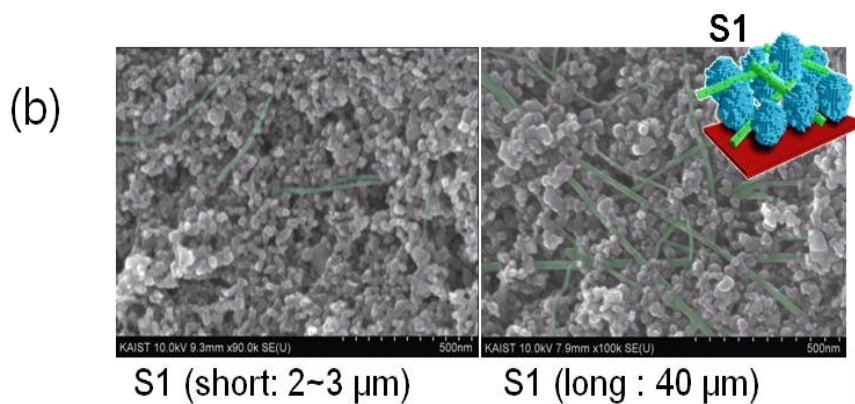
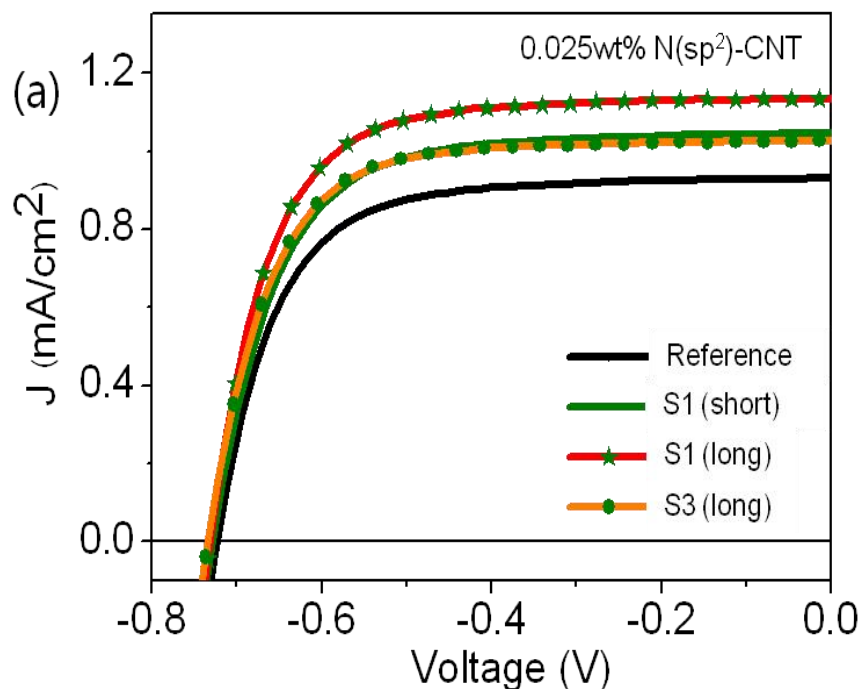
Fig. S1 (a) IV curve of a mixed sp^2 - and sp^3 -nitrogen doped carbon nanotube incorporated DSSC, (b) TEM image of sp^2 - and sp^3 -nitrogen doped nitrogen doped carbon nanotube. N 1s XPS spectra can be divided by three Lorentz fits: 1) 398.2 eV matches with a pyridine-like carbon nitride structure ($N(sp^3)$);¹; 2) 401.3 eV corresponds to a graphite-like carbon network ($N(sp^2)$);² and 3) 404.8 eV corresponds to molecular N_2 atoms, where the binding energy of 404.8 eV is lower than the original binding energy of 409.9 eV for the free N_2 gas, attributed to the screening effect between N 1s core hole and matrix.³ $N(sp^2)$ peak was mainly observed from the $N(sp^2)$ CNT condition (Fig. 1b). On the other hand, as the N concentration increases, we find that a $N(sp^3)$ peak along with the $N(sp^2)$ peak shows up.



10

15

Fig. S2 (a) J - V , and (b) SEM images of DSSCs based on short ($2\sim 3\mu\text{m}$) and long ($\sim 40\mu\text{m}$) $\text{N}(sp^2)$ -CNT mixed TiO_2 photoelectrodes at 0.025% (w/w) on **SI** arrangement. (c) diffusion coefficient of photoelectrons for cells incorporated with $\text{N}(sp^2)$ -CNTs of different lengths.



(c) Electrode Type	Electron diffusion coefficient, D_n (cm^2/s)
Reference	4.22×10^{-6}
S1 (Short)	2.70×10^{-5}
S1 (Long)	4.23×10^{-5}

Concentration effect of CNT and N(sp²)-CNT in structure **SI**, **SII**, **SIII**

The variation of short circuit current density (J_{sc}) and open circuit voltage (V_{oc}) are significantly dependent on the electrode structure and concentration of pristine carbon nanotubes (CNTs) in the mesoporous TiO₂ layer. At 0.025 %, the optimum level of nanotubes in the photoanode, J_{sc} for **SI**, **SII**,
5 and **SIII** increased by up to 19, 9, and 17%, respectively. This can be attributed to the superior charge collection and transport properties of CNTs. On the other hand, V_{oc} was almost similar to that of the reference system for **SIII**, while **SI** and **SII** displayed a decrease of V_{oc} significantly up to 30 mV as shown in **Table S1**. The formation of surface states or traps at interfaces of FTO|CNTs and TiO₂|CNTs (denoted as **S_{FC}** and **S_{TC}**, respectively) was expected as a main source of V_{oc} decay. Both **S_{FC}** and **S_{TC}**,
10 formed energetically below the Fermi level of FTO and the conduction band edges of TiO₂ (**E_{CB,TiO2}**), respectively, facilitated the back reaction of electrons at the photoanode with I₃⁻ in electrolyte. The contribution of **S_{FC}**, highly localized at the FTO surface, is most significant in **SII** while it is eliminated in **SIII** arrangement by introducing a thin TiO₂ buffer layer. However, **S_{TC}** is homogeneously distributed over the mesoporous TiO₂ layer in **SI** and on the upper layer in **SIII**, while
15 the population of this state is highly localized on the FTO surface in **SII** arrangement.

The significant decrease in cell performance was observed on a higher concentration of CNTs than the optimized level (0.025%) with respect to TiO₂. The pronounced decrease in the J_{sc} was observed along with an additional decrease of V_{oc} that was slightly greater than with the optimized CNT content of nanotubes. This was generally attributed to the blocking or attenuation of light absorption due to the
20 inherent dark nature of CNTs and the increased contribution of surface states (**S_{FC}** and **S_{TC}**) within the photoelectrode. However, the effect of the nanotubes was not so prominent below the optimum CNT level mostly due to the very low densities of both surface states.

For the higher concentrations of N(sp²)-CNTs (0.9 and 0.2 wt %), the V_{oc} decay were not significant in **SI** and **SIII** arrangements and they remained almost similar to the value of the reference system. J_{sc}
25 in **SIII** was preserved while it decreased in **SI** as the concentration of nanotubes increased.

The structure (SI, SII, SIII) – efficiency correlation

However, it also should be noted that 19 and 21% enhancements for the power conversion efficiency were obtained on **SI** and **SIII** arrangements, respectively, while **SII** showed no notable improvement or decrease in the overall cell efficiency.

$S_{\text{FC(N)}}$ was highly localized at the FTO surface and the contribution of this surface state was most significant in the **SII** arrangement while it was being removed in **SIII** by introducing a thin TiO_2 buffer layer. Meanwhile, the population of $S_{\text{TC(N)}}$ was only extremely localized on the FTO surface in the **SII** arrangement. However, it was homogeneously distributed over the mesoporous TiO_2 layer in **SI** and on the upper layer in **SIII**. In addition, it was found that $S_{\text{FC(N)}}$ still induced V_{oc} drop by up to ~10 mV in **SI** compared with **SIII**, even though the contribution of this surface state to the J - V characteristics in **SI** was insignificant compared to that of $S_{\text{TC(N)}}$ (**Table S2**). Therefore, a notable drop of V_{oc} in **SII** was attributed to the highly concentrated $S_{\text{FC(N)}}$ such that it resulted in significant electron loss. In this case, the back electron transfer to the electrolyte was demonstrated to be more favourable as confirmed through electrochemical impedance spectroscopy (EIS) measurements. On the other hand, electron collection could be increased by providing cascade type electron transfer channels at the $\text{FTO|N}(sp^2)\text{-CNTs|TiO}_2$ interfaces through $S_{\text{FC(N)}}$ and $S_{\text{TC(N)}}$. However, the lack of additional electron collection and transporting channels by $S_{\text{TC(N)}}$ within the mesoporous TiO_2 layer under **SII** arrangement gave no improvement of the overall efficiency. In fact, these results clarify that the overall energy conversion efficiency of DSSCs with $\text{N}(sp^2)\text{-CNTs}$ with more positive Fermi levels compared to pristine CNTs was enhanced irrespective of the spatial arrangement of nanotubes.

The $\text{N}(sp^2)\text{-CNT}$ length effect in DSSC

The $\text{N}(sp^2)\text{-CNTs}$, with an average length of 40 μm , were used to investigate the effect of the elongation of nanotubes. The J - V curves and characteristics parameters are shown in **Fig. S2a** and **S2c**

respectively. The DSSC on longer nanotubes (40 μm) exhibited a 12% higher power conversion than nanotubes of the smaller length (3 μm) while V_{oc} was maintained. This finding implies that longer $N(\text{sp}^2)$ -CNTs did not contribute significantly to the formation of extra surface states, resulting in a significant decay of V_{oc} , but were more effective in enhancing electron transport across the mesoporous TiO_2 layer. This could be explained by the electron diffusion coefficient (D_n) according to Equation 2.⁴

$$D_n = L^2 / (R_t C_\mu), \quad (2)$$

where L is the thickness of the TiO_2 layer. The resistance of electron transport (R_t) and the chemical capacitance (C_μ) at the TiO_2 -electrolyte were obtained from the fitting of EIS data, where the longer nanotubes gave significant decrease of resistance, R_t . The electron diffusion coefficient on the longer channel is 66% higher than that on the shorter channel (**Fig S2c**), thus implying that the incorporation of longer nanotubes contribute to enhance the photocurrent by increasing the overall conductivity of the electrode. The SEM image, shown in the **Fig. S2b**, support the possibility of enhancement of the photocurrent due to conductivity increase by longer nanotubes being extended deeper and wider throughout the TiO_2 mesoporous layer.

Reference

- 1 S. Stafstrom, *Appl. Phys. Lett.* 2000, **77**, 3941.
- 2 S. Souto, M. Pickholz, M. C. dos Santos, F. Alvarez, *Phys. Rev. B* 1998, **57**, 2536.
- 3 F. Esaka, H. Shimada, M. Imamura, N. Matsubayashi, T. Kikuchi, K. Furuya, *J. Electron Spectrosc. Relat. Phenom.* 1998, **817**, 88.
- 4 C. He, L. Zhao, Z. Zheng and F. Lu, *J. Phys. Chem. C*, 2008, **112**, 18730-18733.